Paper No.
640

CORROSION 93
The NACE Annual Conference and Corrosion Show

CO_2 CORROSION OF CARBON STEEL IN TWO-PHASE FLOW

Srdjan Nesic and Liv Lunde

Institutt for energiteknikk
P.O. Box 40
N-2007 Kjeller, Norway

ABSTRACT

In this paper results from the experiments on CO_2 corrosion of carbon steel in two-phase flow are presented. An extensive experimental program has been carried out within the PROFF project initiated in 1989 by the Royal Norwegian Council for Scientific and Industrial Research (NTNF) and cosponsored by a number of companies. Tests were carried out in a gas/water loop which enabled control and regulation of relevant parameters.

Flow rates of gas and water were regulated independently to obtain a number of two-phase flow regimes such as bubble flow and slug flow. In more than 20 long term experiments lasting from one to several weeks each, pH was varied from pH 4 to pH 7 while the temperature was held at 20, 40, 60 and 80°C in different experiments. Corrosion rate was monitored continuously in time with a radiation detection technique. SEM analysis and X-ray analysis of the specimen surface and cross-section was done after each experiment on selected specimens.

It was found that in cases when it is difficult to form protective films flow can have a "positive" role by eroding the iron carbide films which otherwise accelerate corrosion by a galvanic action. In cases when protective films do form (higher pH and higher temperatures, Fe^{++} at saturation or super-saturation) low corrosion rates were obtained - order of 0.1 mm/y. Protective films have in most cases proven to be very resistive to mechanical erosion even in the cases of severe flow conditions caused by slugging and flow disturbances. In some cases damage at the top of the pipe was higher than at the bottom.

Keywords: CO_2 corrosion, two-phase flow, carbon steel, protective films

INTRODUCTION

The Royal Norwegian Council for Scientific Research (NTNF) and a number of companies have jointly financed a large multiphase flow research program (PROFF) in the period 1988 - 1992. One of the main research areas covered was materials and corrosion as related to multiphase oil and gas production. The results presented in this paper are some of the data accumulated over the 4 years of research on CO_2 corrosion of carbon steel in two-phase flow. The final stages of the experimental program are being completed as this paper went into print. It is planned to use the substantial body of new data obtained for creating a mathematical model with a long term goal of developing a predictive model for CO_2 corrosion in multiphase flow.

Many experimental studies on the effect of individual parameters on CO_2 corrosion such as pH, CO_2 pressure, temperature, have been conducted in the past. On the basis of these studies empirical parameter-models were constructed and have been the main tool used by the industry to predict the corrosion rates.

At the Institutt for energiteknikk a very intensive program on CO_2 corrosion has been conducted over the past ten years. The effect of CO_2 partial pressure, temperature, pH, flow conditions, iron carbonate solubility, film formation, alloying elements and heat treatment has been studied in loop tests under high pressures and different temperatures. From the data released so far [1-4] one can summarize the effect of individual parameters as follows.

- **pH** - Increased pH gives lower corrosion rate due to lower availability of H^+ ions and lower rate of the hydrogen reduction reaction. Higher pH also means lower solubility of iron carbonate giving a higher probability for protective film formation.

- **CO_2** - Higher CO_2 partial pressure gives a higher corrosion rate due to a reduction in the pH and due to the increased rate of the carbonic acid reduction reaction.

- **Temperature** - Higher temperature gives a higher corrosion rate due to acceleration of electrochemical and chemical reactions at elevated temperatures. However, precipitation rates also increase thus at high temperatures protective films form more easily and can lead to a reduction in the corrosion rate.

- **Iron carbide** - Presence of iron carbide (Fe_3C) in the surface film is considered to increase the corrosion reaction by selectively increasing the cathodic reaction rate (galvanic effect).

- **Iron carbonate solubility** - When the solubility limit for iron carbonate ($FeCO_3$) is reached or exceeded it precipitates onto the metal surface forming a protective film. Due to fact that precipitation does not occur instantaneously when thermodynamic saturation is reached it is possible to exceed this limit in a corroding system (super-saturation). The degree of super-saturation is a function primarily of the metal-to-water ratio, temperature and pH.

- **Protective films** - Iron carbonate films are considered to be protective in many cases and reduce the corrosion rate by limiting the transport of chemical species involved in the electrochemical reactions.

- **Flow** - Higher flow rate usually gives higher corrosion rates by increasing the transport rates of reacting species to the metal surface and by preventing or destroying protective films. Under some conditions higher flow rates mean lower corrosion rates when iron carbide films are removed.

Most previously available studies on CO_2 corrosion in flowing systems outside the present project have been conducted at single phase (liquid) flow conditions. Even then many findings were ambiguous due to the large number of parameters involved interacting in a very complex way. However, new challenges are not waiting for us to resolve the old ones, so the question of CO_2 corrosion in two-phase flow (gas/liquid) systems has been addressed in the present study.

EXPERIMENTAL RESULTS

Due to the fact that our present understanding of CO_2 corrosion is not complete, more experimental evidence is needed to clarify the effects of some important parameters. It is however impossible to decouple the influence of individual parameters from others so the experiments that have been conducted within the PROFF project included very careful monitoring and automatic regulation of the key parameters. This is not the case with many studies that appear in literature. For example, it is of little use to perform a CO_2 corrosion experiment at a certain carefully monitored pH, CO_2 partial pressure, flow rate and temperature but not follow the amount of dissolved iron carbonate in the water which is crucial for the protective film formation.

The loop

The experimental flow loop that was used in the present study is shown on Figure 1 and Figure 2. There were a few major requirements which determined the layout of the experimental setup:

- accurate and independent control of flow parameters for each phase,

- careful monitoring and control of water chemistry and temperature and

- stable and reliable automatic operation of the loop for extended periods of time (up to several weeks).

The propulsion system is shown on Figure 1. Liquid is transported by a canned centrifugal pump. The pump motor is cooled and lubricated with the loop water avoiding the risks of contamination of the water with cooling liquids and lubricants. The pump capacity is 14 m^3/h at a liquid head of 50 m. It is made from AISI 316 stainless steel and can operate at pressures up to 25 bar and temperatures of 100 °C. Gas is transported by an ejector system. This setup was selected to avoid more expensive solutions including air tight compressors.

There are two tanks made from carbon steel lined with butyl rubber. The low pressure tank is a separator for the two-phase mixture returning from the test section. The high pressure tank separates the two phases coming from the ejector so that they can be independently metered and introduced into the test section.

The two-phase mixture flows through a horizontal pipe (ID 32 mm), 14.5 m long (entry length - 450 diameters) leading into the horizontal test section. All pipes and other components of the loop (valves, fittings) are made from AISI 316 stainless steel. The inclination of the pipe can be adjusted with the accuracy of 0.1 mm/m (0.01°) what can be of great importance in stratified two-phase flow. Optionally additional test sections with half the cross section (ID 22 mm) and double the cross section (ID 50 mm) can be added to the loop in series. In both cases appropriate entry lengths of 300-400 diameters are allowed for. Since corrosion experiments typically last a few weeks, accumulation of data is a slow process so that measuring corrosion rates for three velocities simultaneously is very beneficial. Altogether there is five locations where the specimen racks can be introduced enabling continuous corrosion monitoring with the radioactive technique, as explained later.

The specimen rack can contain anywhere from a few to fifty tubular specimens (wall thickness 0.5 mm) which are embedded into Teflon. This prevents corrosion from the outer surface of the specimen and electrically isolates them from the loop. The Teflon rings with the specimens are then embedded into a stainless steel specimen rack as shown on Figure 2 to enable withstanding of high pressure.

Water Treatment

Water chemistry is one of the most important factors affecting the corrosion rate so a lot of attention has been given to this problem. In CO_2 corrosion experiments it is essential to maintain very low O_2 concentration in the water. Water preparation included: filtering, deionization, keeping at 90 °C at least for 12 hours and then boiling for another hour in special purpose tanks. Once in the experimental tanks CO_2 and N_2 are added to the water. Pressure is then reduced to strip the remaining oxygen with rapidly developing CO_2 bubbles. After this procedure is repeated several times O_2 concentrations as low as a few ppb are obtained.

The pH of the water is controlled in several ways. The pH depends on the CO_2 partial pressure, amount of dissolved Fe^{++} ions and addition of other chemicals ($NaHCO_3$ has been used to increase the pH). The Fe^{++} concentration is controlled by an iron generator (for increasing Fe^{++} concentration) and an ion exchanger which can substitute the Fe^{++} in the solution by H^+ or Na^+ ions. The ion exchanger is controlled with a pH meter enabling continuos and automatic maintenance of unchanged pH and Fe^{++} concentration for extended periods of time. Other chemicals such as $NaHCO_3$, NaCl, acids, bases and inhibitors can be added continuously to the loop with an accurate piston metering pump.

Control and Monitoring Equipment

A concise list of all the parameters monitored and regulated, is given in Table 1. The gas flow rate is measured with a rotameter (variable area flow meter). The liquid flow is metered by a Venturi-Cone. In order to qualitatively characterize the two-phase flow a transparent section is placed after the test section. Pressure drop measurements are performed on the straight portion of the pipe enabling

determination of average wall-shear stress. In case of slug flow pressure fluctuations are measured on the pipe wall in order to determine the slug frequency and amplitude.

The water temperature is kept constant within 0.1 °C in the range 10 - 100 °C. The pH is measured with two independent electrodes in order to register a possible drift. When the discrepancy in the readings on the two pH meters is larger than 0.1 the electrodes are checked and recalibrated and eventually replaced. The measurements of the pH are used to automatically activate the ion exchanger maintaining a stable pH for long periods of time. The O_2 content is measured continuously and kept below 20 ppb throughout the experiment. Samples of the loop water are taken at least once a day to monitor the amount of dissolved CO_2 and the concentration of Fe^{++}.

The corrosion rate is measured by recording the specimen weight loss and the wall-thickness reduction prior and after the experiment. In addition, the corrosion rate is recorded continuously with a radiation technique (Figure 2). The method is based on measurement of the gamma rays emitted from one of the specimens which is neutron activated (details of the technique are given elsewhere [5]). The corrosion rate is determined by the loss of radioactivity due to removal of the metal by the corrosion reaction. The technique in the present experiments had the sensitivity below 0.1 mm/y. It is possible to selectively activate only the top or the bottom of the specimen and in that way distinguish between the corrosion rates at different locations. After the exposure the specimens are inspected by a scanning electron microscope (SEM) and the X-ray diffraction technique.

RESULTS

When conditions for protective film formation are favorable it is important to allow for long term experiments as it takes a few days for a stable protective film to form, all other conditions being unchanged. Thus most of the performed experiments lasted one or more weeks. There are many parameters that can be varied in CO_2 corrosion experiments and the number of combinations is even larger. In performed experiments ranges were selected as suggested by field measurements and are listed in Table 2.

In the first part of the experimental program two specimen racks were used each containing three tubular specimens (ID 32 mm). In each rack the middle specimen was activated and its corrosion was followed with the radiation technique (Figure 2). The difference was that in one rack the specimen was activated only in the top portion and in the other rack only in the bottom. In that way it was possible to follow whether the corrosion rates differed at the top and bottom of the pipe. The specimens were machined from a seamless tube made of normalized St.52 carbon-manganese steel with a yield strength of 406 N/mm^2.

Non-protective films

When steel corrodes surface films with iron carbide are often present. Iron carbide is not a corrosion product in a classical sense as it comes from the parent metal. Iron carbide might be seen as a skeleton of the metal which remained after the corrosion process removed the rest of the metal. Iron carbide films are often labeled as the "uncorroded portion of the metal". Such films are very porous and

non protective. In all our experiments at T=20°C we have encountered surface films that consisted predominantly of iron carbide.

The most significant effect of flow was noticed in the experiments done at low temperatures (T=20°C). At these temperatures it is difficult to form protective iron carbonate films and a high Fe^{++} super-saturation is possible. After the exposures it was observed that the surface was covered with iron carbide films The iron carbide films appeared to be very susceptible to erosion by the flow. It is interesting to notice that this is a mechanical effect of the flow that affects the electrochemical processes and is not related to mass transfer. For an experiment done at T=20 °C, pH 5.3 with a high Fe^{++} super-saturation, the development of the corrosion rate in time is shown on Figure 3. Flow was initially single-phase (water) and a steady increase in corrosion rate was recorded which can be explained by the growth of an iron carbide film. No difference in corrosion rate between pipe top and bottom can be noticed in this period. The accidental stop in the flow that occurred for 2.5 hours on day 6 of the experiment, caused a radical drop in the corrosion rate. This can be explained by the fact that under stagnant conditions with the high Fe^{++} super-saturation, despite the low temperature, favorable conditions were reached for forming of iron carbonate films with protective properties. After the restart of the flow the protective films were gradually destroyed and the corrosion rate increased steadily in the same way that it did prior to the stop. However, when after 26 days the flow regime was changed to slug flow, the corrosion rate at the top of the pipe dropped to only half the value of that at the bottom. Subsequently, the corrosion rates of both the top and the bottom continued increasing but at different levels. The experiment was stopped after 33 days without reaching a steady state although it might be expected that the final corrosion rate would be close to 5 mm/y which is a prediction made with the IFE-COR (V 1.0) corrosion model. SEM images show the metal surface covered predominantly with a flaky iron carbide film (Figure 4).

If we accept the assumption that iron carbide films can accelerate corrosion, then in the experiment shown on Figure 3 the difference in the corrosion rates of the top and the bottom of the pipe after the introduction of the two-phase slug flow can be explained. The iron carbide film at the top of the pipe was eroded faster than the one at the bottom where there are smaller pressure and shear stress fluctuations due to slugging. Measurements of the wall pressure fluctuations due to slugging that were performed revealed that for the flow regime under consideration slug frequency was typically 1 Hz while the magnitude of the oscillations was of the order of 500 Pa. The latter is very significant when compared to the value of the mean wall shear stress that is an order of magnitude lower (50 Pa). This shows that slugging exerts large additional mechanical forces onto the film and it is not strange that the weak iron carbide film could not resist them.

The stated assumption was further confirmed by looking at the SEM images of the cross section of the attacked specimens (Figure 4). All of them exhibited films that consisted predominantly of iron carbide. The iron carbide film was always thinner on the top of the specimen (0 - 20 μm) than on the bottom (20 - 100 μm). At higher pH more flow-resistive films with somewhat more protective properties were formed, most probably due to precipitation of iron carbonate. The role of iron carbonate was both to reinforce the flaky iron carbide structure and to offer some protection through increased resistance for diffusion of the species involved in the electrochemical reactions.

Protective films

Formation of protective films is crucial for survival of carbon steels in CO_2 containing aqueous environments. Iron carbonate films usually have some protective properties. However, their formation is a complex function of many parameters such as pH, temperature and Fe^{++} solubility. The combined effect of pH and Fe^{++} concentration on the formation of protective films is shown on Figure 5. In that experiment slug flow was maintained, temperature was T=40 °C , Fe^{++}= 70 ppm and $p_{CO_2} = 1.2\,bar$. In the beginning of the experiment pH 5 was set. The corrosion rate increased steadily during the first few days of the experiment reaching a high value of 8 mm/y. This indicates that there were no protective films forming. The increase in the corrosion rate can be attributed to growth of iron carbide (Fe_3C) films. After one week the iron generator was activated and iron ion concentration was increased to a very high level (Fe^{++}=400 ppm) what is in the supersaturated region. The pH was increased accordingly to near pH 6. The corrosion rate decreased rapidly to 3 mm/y. Since favourable conditions for iron-carbonate precipitation were reached protective $FeCO_3$ films formed resulting in a further decrease in the corrosion rate. This reduction was gradual (4-5 days) as protective film formed. The final corrosion rate was in the range 0.1 - 0.5 mm/y and stayed at that level for the last 10 days of the experiment. No systematic difference between the corrosion rates at the top and bottom of the pipe could be noticed. The appearance of the surface films in this experiment is illustrated on the SEM image of the specimen cross section - Figure 6 . It can be seen that next to the metal surface there is a loose very porous film consisting of iron carbide sprinkled with iron carbonate crystals. It is probable that this film which formed during the first part of the experiment offers no corrosion protection for the metal. At the outer surface there is a dense film consisting mostly of iron carbonate formed in the second part of the experiment at higher pH and Fe^{++} concentration with protective properties.

Flow disturbances

For practical purposes we are interested in cases where protective films are formed and removed selectively by the flow causing severe localized attack. Thus, to study the effect of flow disturbances, high temperature T=80°C, pH 5.5*, and Fe^{++} supersaturation were selected. This is the case when it is probable that protective films will form and subsequently might be removed locally.

Besides the existing specimen rack described previously, two new specimen racks were added: one containing a test section with a constriction and an expansion geometry (Figure 7) and the other test section with a 2 mm protrusion and two grooves with 2 mm and 4 mm gap (Figure 8). These are some of the most important generic geometry that are often found in practice. The two new test sections were constructed from a set of rings of two different diameters and different length in order to enable weight loss detection of corrosion profiles along the test section and identification of critical spots where localized attack was highest. In addition two of the rings were activated (indicated with a ☢ flag on the Figure 7 and Figure 8) so that development of the corrosion rate in time could be followed with the radioactive technique. The two cross sections of the pipe (22.5 mm and 32 mm in diameter) were selected to give a velocity ratio of 2:1.

---

* The pH 5.5 was achieved by adding sodium bicarbonate.

In most experiments corrosion rates dropped in a few days from a few millimeters per year to a tenth of a millimeter per year or less (Figure 9). Due to high supersaturation of Fe^{++} ions protective films formed and were not removed subsequently, at least not in whole. In all experiments SEM analysis revealed that most of the attack was concentrated in pit-like cavities (Figure 10). A very thin layer (order of 1 μm) of iron carbonate was covering and protecting the rest of the surface. Antimony was often found in this thin surface film. It was discovered later that antimony was dissolving from a pump bearing and this was eliminated. The exact role of antimony in the corrosion process is not yet understood, but it appears that antimony improved the film protective properties. In one experiment a number of specimens was analyzed by SEM. Most of them were selected in pairs from the same flow geometry - one having a high and the other a low corrosion rate. In all cases the character of attack was the same - the thin corrosion film and the pits. However, the specimens that were located in the areas with increased turbulence as a rule had higher corrosion rates measured with the weight loss technique and more numerous and deeper pits.

When first pits were noticed it was suspected that their formation might be connected with some aspect of the metal microstructure. One of the pitted specimens was etched and observed under the microscope (Figure 11). No connection could be seen between the shape of the perlitic bands and the onset of the pits. In some cases the pits were connected to an occurrence of inclusions in the metal. However, this was more an exception than a rule.

The pit-like character of the attack observed on most SEM images of the surface can be tentatively explained as follows. Due to high Fe^{++} supersaturation protective iron films formed rapidly (within a day or two) and reduced the corrosion on most of the specimen surface. At locations exposed to high turbulence levels or close to some imperfections in the parent metal surface, the protective film was damaged and localized attack was initiated. The attack propagated due to a galvanic cell that was established similar as in crevice corrosion. It is then straightforward to explain that in areas with increased near-wall turbulence more damage was inflicted in the protective films and more numerous pits were formed.

In one of the experiments in this series water conditions were changed to provoke a larger corrosion effect. The first measure taken: reduction the pH from 5.5 to 5.0 did not affect the average corrosion rate significantly as supersaturation of Fe^{++} was maintained and protective films remained stable. When subsequently the Fe^{++} concentration was reduced close to the saturation level, still very little change in the corrosion rate was observed (Figure 12). This can be explained with the fact that the potential for dissolution of protective films was small and even if the film started dissolving it was a very slow process. However, when the Fe^{++} concentration was reduced far below the saturation limit corrosion rates increased due to the rapid dissolution of protective films. SEM analysis suggested that this dissolution proceeded faster at the top of the pipe and close to geometrical irregularities, both being the areas with increased turbulence and mass transfer. On all SEM images obtained there is virtually no protective films on the surface (Figure 13).

Two-phase flow

One of the aims of this study was to capture the effect of (two-phase) flow on corrosion. All other parameters that affect corrosion rate other than the flow rate were kept more or less constant in one set of experiments. From the range of flow regimes studied and the five different geometries a

large number of comparisons can be made. To illustrate the dominant trends we have selected a few comparisons where the effects are the clearest.

On Figure 14 the corrosion profiles for flow through a sudden constriction are compared for the case of single-phase water flow and two-phase slug flow. Since the turbulence level in case of slug flow is higher it is not a surprise that the whole profile is somewhat elevated compared to the one for water flow. In both cases there was some effect at the constriction corner (although not very large). However, in the slug flow experiment 3 % NaCl was added and pH was 0.2 units lower so this may account for the somewhat larger effect. In Figure 15 corrosion profiles are compared for flow over the 2 mm and 4 mm grooves and the protrusion. Data were taken from one experiment with single-phase flow and one with two-phase flow. Again a consistent increase in the corrosion rate is evident for the case of slug flow.

CONCLUSIONS

1. When solubility of Fe^{++} in water is exceeded favorable conditions are reached for precipitation of iron carbonate. Iron-carbonate films usually have protective properties and reduce the corrosion rate by offering greater resistance for diffusion of species involved in the electrochemical reactions.

2. At low temperatures (T=20°C) it is difficult to form fully protective iron carbonate films under flow conditions even when the iron carbonate concentration exceeds the thermodynamic saturation limit. This was found over a range of pH (5.1 - 6.8). At higher pH some iron carbonate precipitated but offered little protection. Its main role was to reinforce the fragile iron carbide film.

3. At higher temperatures (T=80°C) protective films formed more easily when saturation of Fe^{++} was reached or exceeded.

4. The protective iron carbonate films once they formed appeared to be very robust and resistive to severe flow conditions. It was found that slug flow conditions with its high fluctuating wall forces did not cause significant damage to these films, or at least not more than single phase flow. Somewhat higher attack was recorded at the top of the pipe.

5. When protective films formed fast, localized corrosion was initiated which then developed into a pit-like attack. It is hypothesized that the initiation of these pits is connected to intense wall forces exerted by the flow and/or by faults in the parent material.

6. In most cases highest corrosion rates were found in the vicinity of the flow disturbances.

7. The iron carbide films that are inevitably present increase the corrosion rate. However they are very susceptible to the flow conditions and can be eroded by the flow. The change to slug flow can cause a rapid erosion of the iron carbide layer at the top of the pipe giving a reduction in the corrosion rate.

ACKNOWLEDGMENT

The support of this research by the Royal Norwegian Council for Scientific and Industrial Research (NTNF) and the following parties is greatly acknowledged: Aker Engineering A/S, Amoco Norway Oil Company, Amoco Production Company, Elf Aquitaine Norge, Esso Norge A/S, Exxon Technology, Framo Eng. A/S, Kværner A/S, NAT, Norsk Hydro A/S, Norske Shell A/S, Saga Petroleum A/S, Shell International Petroleum, Statoil, Total Paris and Total Norge A/S.

REFERENCES

1. K. Videm and A. Dugstad , "Effect of Flow Rate, pH, Fe^{2+} Concentration and Steel Quality on the CO_2 Corrosion of Carbon Steels", Corrosion/87, paper no. 42, (Houston, TX: NACE, 1987).

2. K. Videm and A. Dugstad , Materials Performance, 28, 3 (1989): p. 63.

3. K. Videm and A. Dugstad , Materials Performance, 28, 4 (1989): p. 46.

4. A. Dugstad , "The Importance of $FeCO_3$ Supersaturation on the CO_2 Corrosion of Carbon Steels", Corrosion/92, paper no. 14, (Houston, TX: NACE, 1992).

5. A. Dugstad and K. Videm, "Radioactive Techniques for Corrosion Monitoring", Corrosion/89, paper no. 159, (Houston, TX: NACE, 1989).

TABLE 1.

EXPERIMENTAL PARAMETERS MONITORED, LOGGED AND REGULATED

Parameter	Monitored continuously	Logged by a computer	Automatically regulated
Gas flow rate	yes	yes	no
Liquid flow rate	yes	yes	no
Total pressure	yes	yes	no
CO_2 partial pressure	yes	no	no
pH	yes	yes	yes
Temperature	yes	yes	yes
O_2 concentration	yes	no	no
Fe^{++} concentration	yes	no	yes
Slugging	no	yes	no
SEM analysis	no	no	
Corrosion rate (measured weight loss)	no	no	
Corrosion rate (radioactive technique)	yes	yes	

TABLE 2.

RANGES OF PARAMETERS USED IN THE EXPERIMENTS.

Parameter		**Range**
Flow regime		single-phase stratified slug bubble
Superficial gas velocity	U_{sg}	0 - 3 m/s
Superficial liquid velocity	U_{sl}	1 - 3 m/s
Total pressure	p_{tot}	4 - 6 bar
Partial pressure of CO_2	p_{CO_2}	1 - 2 bar
Iron ion concentration	$[Fe^{++}]$	0-500 ppm
Temperature	T	20-80 °C
pH		4 - 7

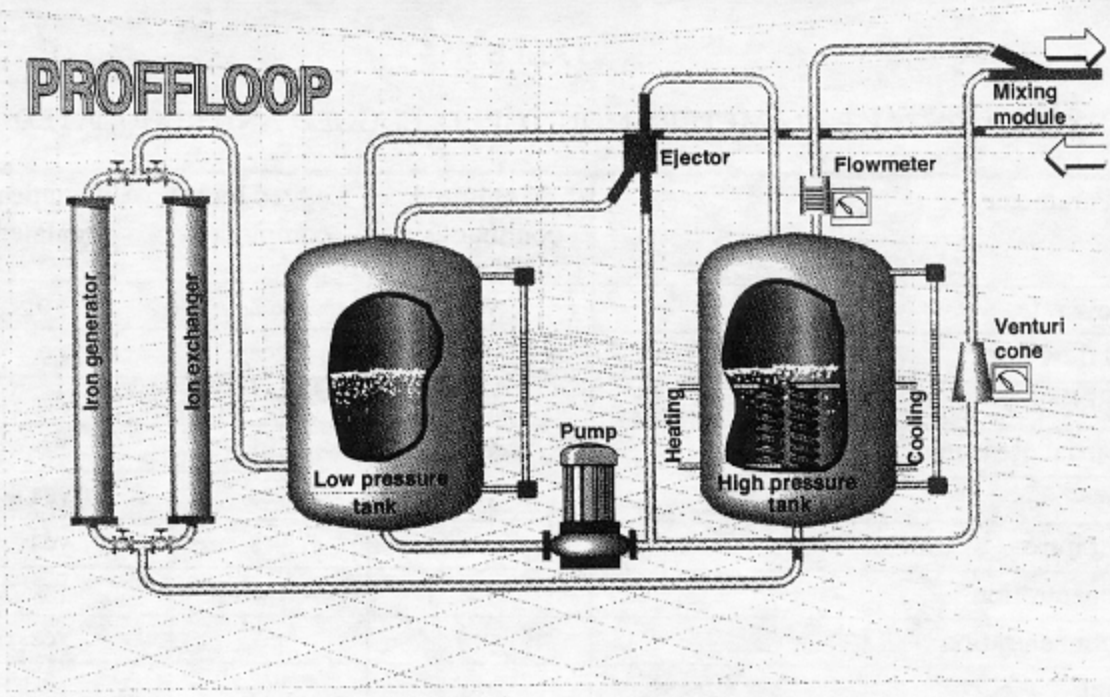

FIGURE 1. The schematic of the experimental flow loop.

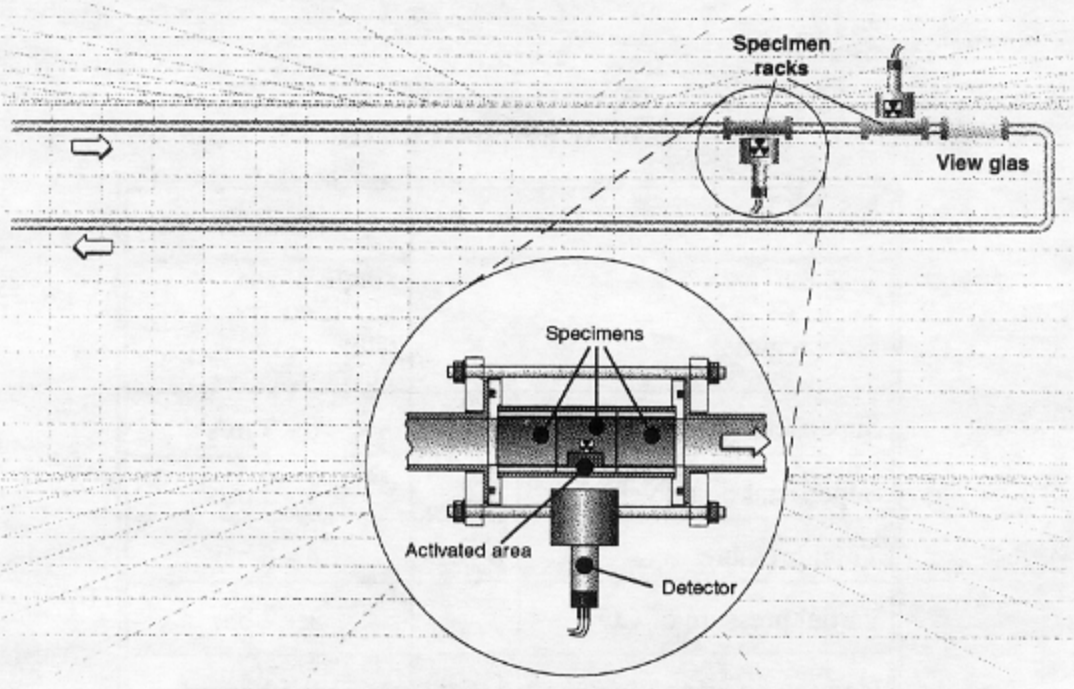

FIGURE 2. The schematic of the test section and the specimen rack.

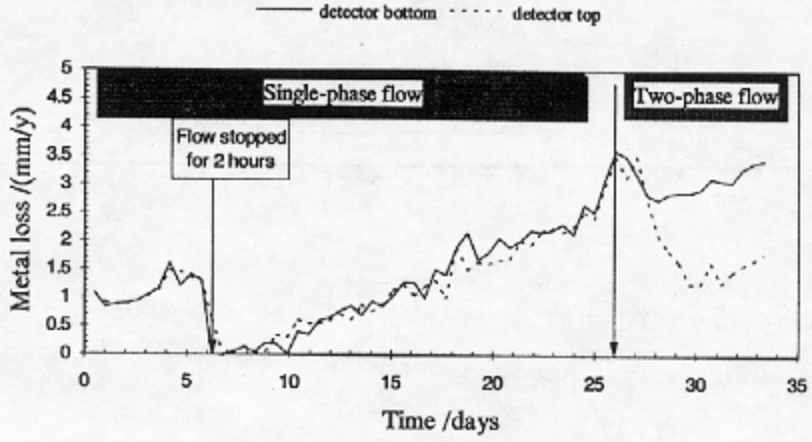

FIGURE 3. Corrosion rate at the top and bottom of the pipe followed with the radiation technique. Specimen exposed to water and slug flow, total velocity U_t=3 m/s, T=20°C, pH 5.3, $p(CO_2)$=1.8 bar, Fe^{++} super-saturated.

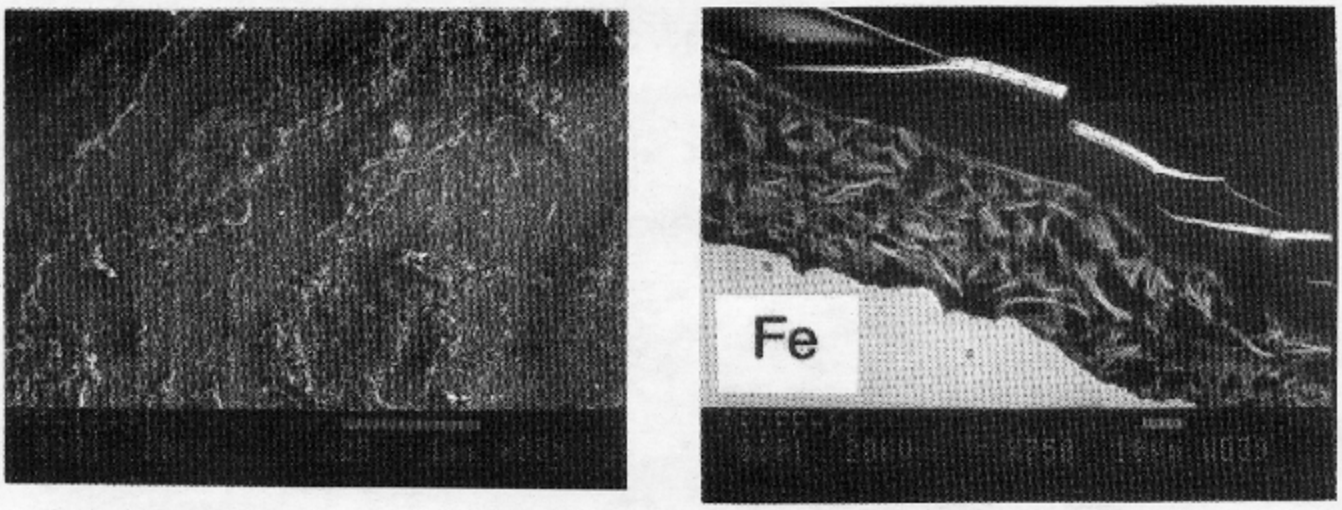

FIGURE 4. SEM image of the: (a) plan view of the specimen surface (magnification × 25); (b) cross section of the surface film (magnification × 750); after exposure to water and slug flow; total velocity U_t=3 m/s, T=20°C, pH 5.3, $p(CO_2)$=1.8 bar, Fe^{++} super-saturated.

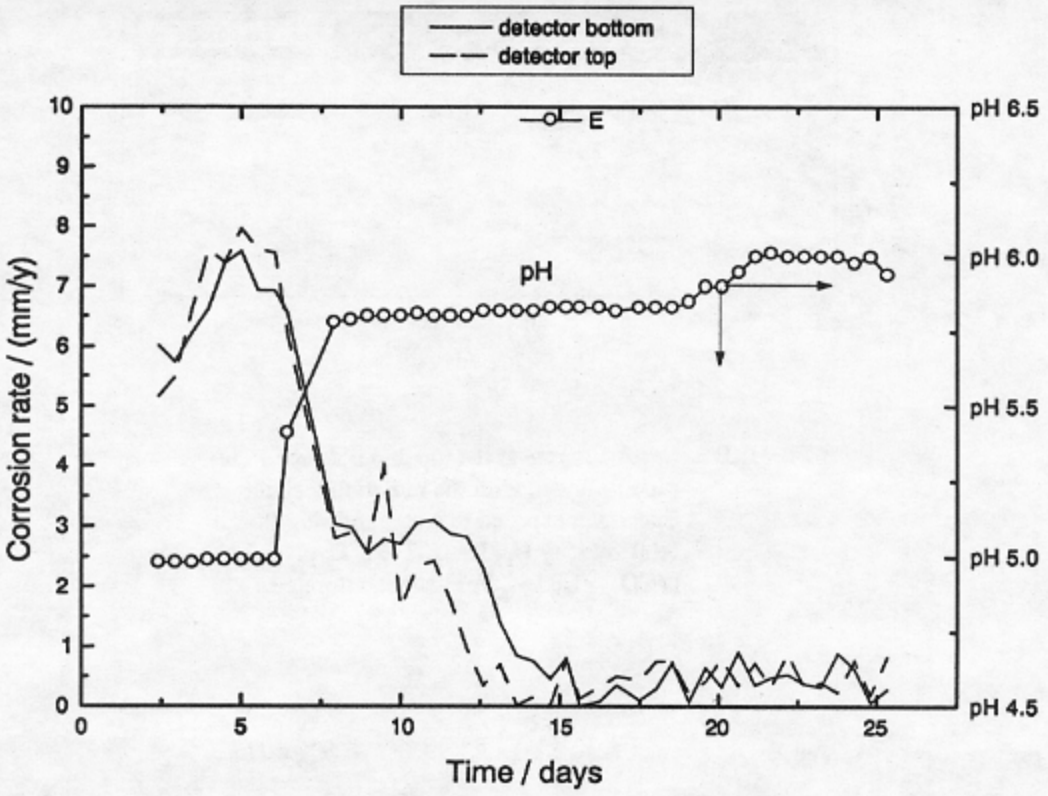

FIGURE 5. The effect of pH on the corrosion rate.

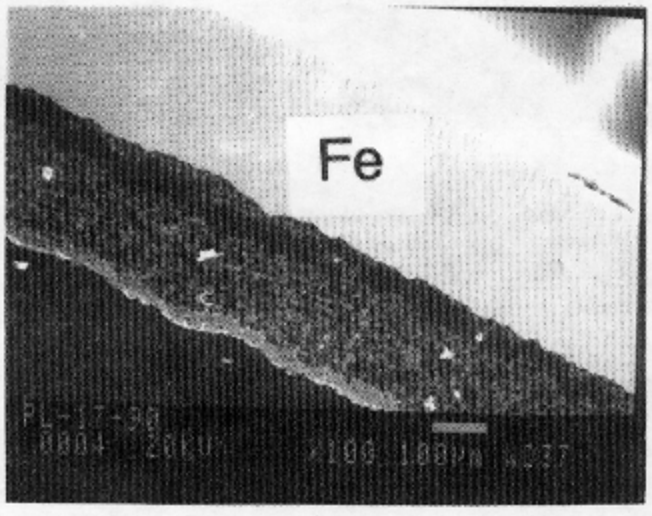

FIGURE 6. The SEM image (magnification ×100) of the cross section of the specimen after exposure to T=40 °C, Fe^{++}= 70-400 ppm and p_{CO_2} = 1.2 *bar*, pH 5-6.

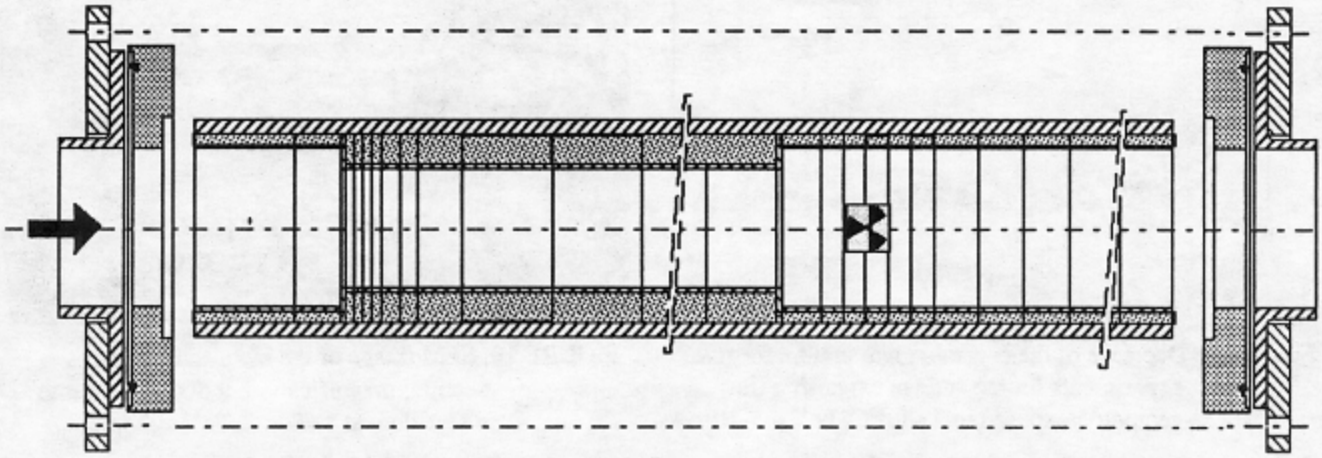

FIGURE 7. Specimen rack with a sudden constriction and expansion

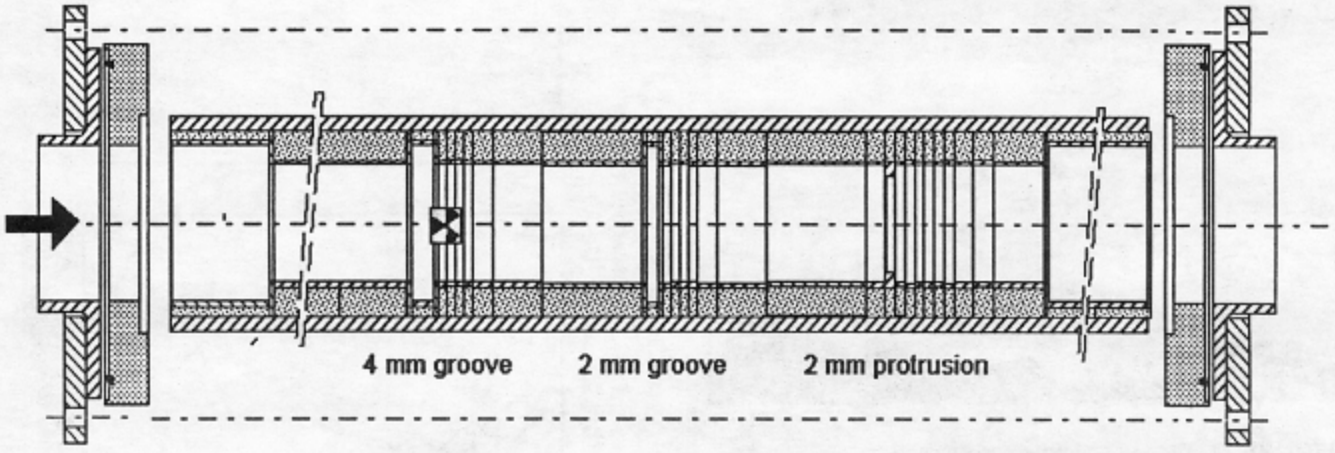

FIGURE 8. Specimen rack with the 4 mm and 2 mm grooves and the 1.5 mm protrusion.

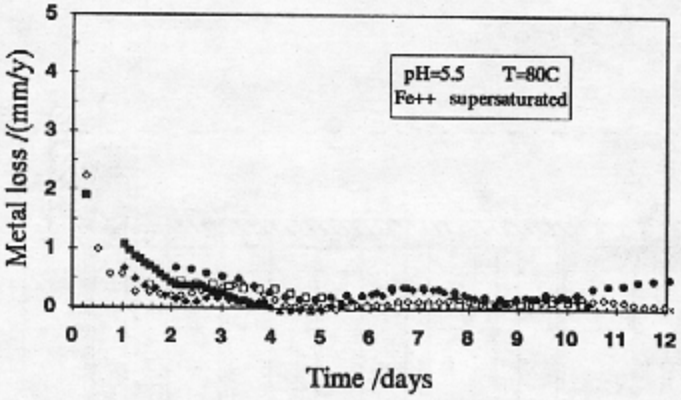

FIGURE 9. Decrease of the corrosion rate in time for five experiments for the sudden expansion flow geometry; exposed to T=80 °C, Fe^{++}= 5-10 ppm, p_{CO_2} = 1.8 *bar*, pH 5.5.

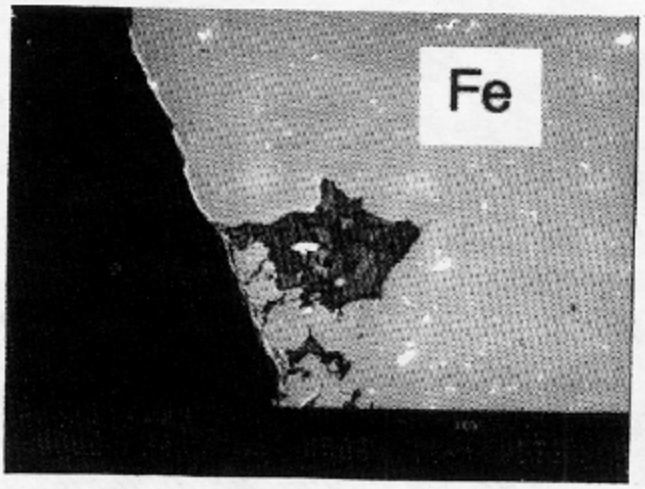

FIGURE 10. SEM image of the metal surface cross section; magnification: × 500; exposed to water flow at T=80 °C, Fe^{++}= 6 ppm, p_{CO_2} = 1.8 *bar*, pH 5.5.

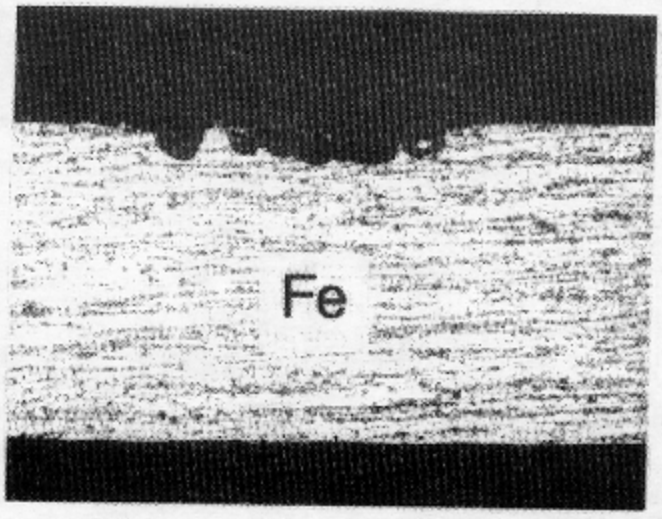

FIGURE 11. Etched specimen cross section; magnification: × 100; exposed to water flow at T=80 °C, Fe^{++}= 7 ppm, p_{CO_2} = 1.8 *bar*, pH 5.5.

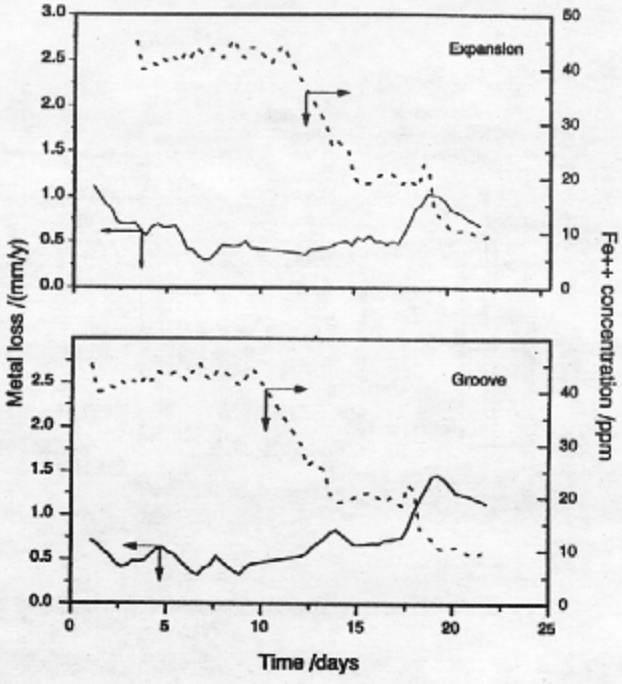

FIGURE 12. Time plots of the corrosion rate as a function of Fe^{++} concentration in slug flow.

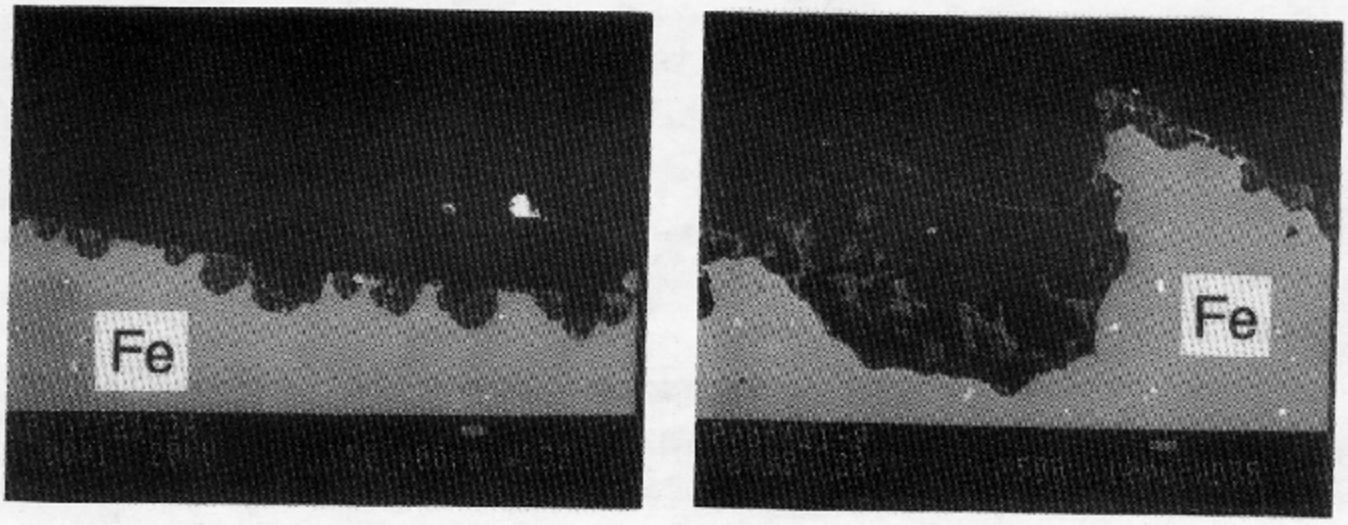

FIGURE 13. SEM images of the specimen cross section; (a) magnification: × 50; (b) magnification: × 500; after exposure to slug flow at T=80 °C, Fe^{++}= 10-40 ppm, p_{CO_2} = 1.8 *bar*, pH 5.0.

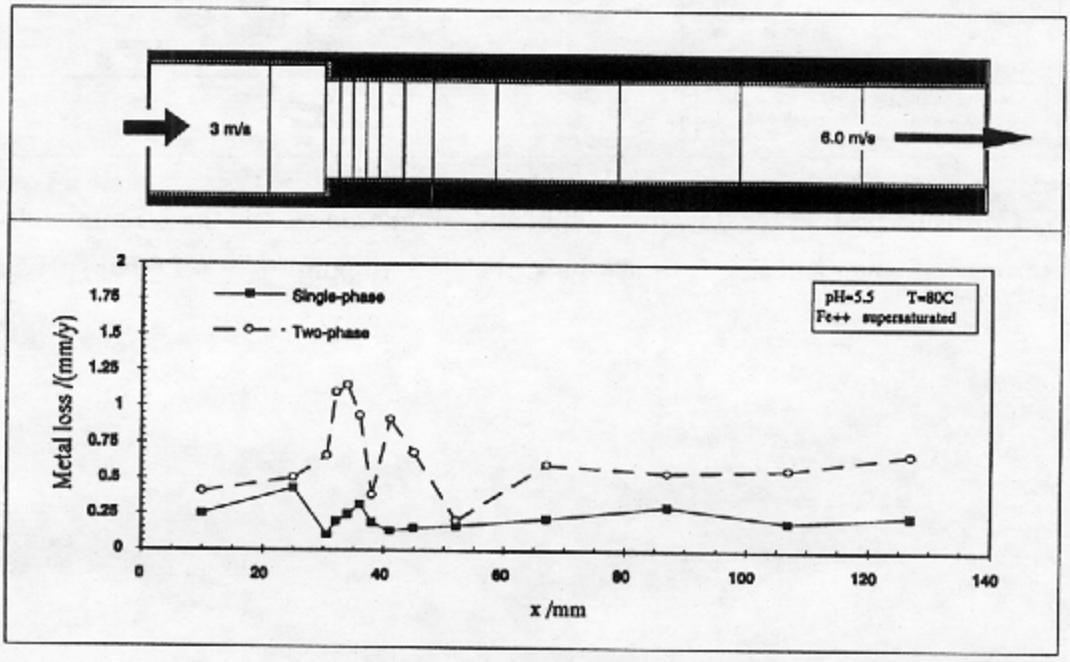

FIGURE 14. Corrosion profiles for flow through a sudden constriction for the case of water and slug flow; T=80 °C, Fe^{++}= 5-10 ppm, p_{CO_2} = 1.8 *bar*, pH 5.5.

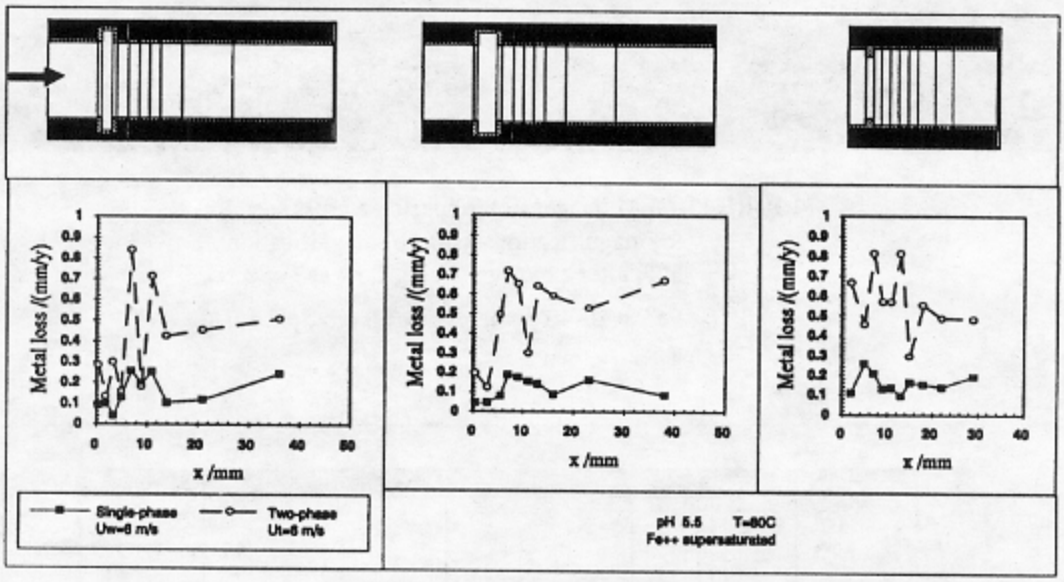

FIGURE 15. Corrosion profiles for flow over 2 mm and 4 mm grooves and the 1.5 mm protrusion for the case of water and slug flow; T=80 °C, Fe^{++}= 5-10 ppm, p_{CO_2} = 1.8 *bar*, pH 5.5.